International Institute for
Applied Systems Analysis
Schlossplatz 1
A-2361 Laxenburg, Austria

Tel: +43 2236 807 342
Fax: +43 2236 71313
E-mail: repository@iiasa.ac.at
Web: www.iiasa.ac.at

Working Paper WP-16-026

Characterization and Control of Conservative and Non-conservative Network Dynamics

Matthias Wildemeersch (wildemee@iiasa.ac.at)
Wai Hong Ronald Chan (whrchan@stanford.edu)
Elena Rovenskaya (rovenska@iiasa.ac.at)
Tony Q.S. Quek (tonyquek@sutd.edu.sg)

Approved by

Pavel Kabat
Director General and Chief Executive
Officer, IIASA

December, 2016

Contents

Characterization and Control of Conservative and Non-conservative Network Dynamics

Matthias Wildemeersch, *Member, IEEE,* Wai Hong Ronald Chan,
Elena Rovenskaya, Tony Q. S. Quek, *Senior Member, IEEE*

Abstract

Diffusion processes are instrumental to describe the movement of a continuous quantity in a generic network of interacting agents. Here, we present a probabilistic framework for diffusion in networks and study in particular two classes of agent interactions depending on whether the total network quantity follows a conservation law. Focusing on asymmetric interactions between agents, we define how the dynamics of conservative and non-conservative networks relate to the weighted in-degree and out-degree Laplacians. For uncontrolled networks, we define the convergence behavior of our framework, including the case of variable network topologies, as a function of the eigenvalues and eigenvectors of the weighted graph Laplacian. In addition, we study the control of the network dynamics by means of external controls and alterations in the network topology. For networks with exogenous controls, we analyze convergence and provide a method to measure the difference between conservative and non-conservative network dynamics based on the comparison of their respective attainability domains. In order to construct a network topology tailored for a desired behavior, we propose a Markov decision process (MDP) that learns specific network adjustments through a reinforcement learning algorithm. The presented network control and design schemes enable the alteration of the dynamic and stationary network behavior in conservative and non-conservative networks.

Matthias Wildemeersch is with the International Institute for Applied Systems Analysis (IIASA), Laxenburg, Austria (email: `wildemee@iiasa.ac.at`).

Wai Hong Ronald Chan is with Stanford University, California, USA (email: `whrchan@stanford.edu`).

Elena Rovenskaya is with IIASA and the Faculty of Computational Mathematics and Cybernetics, Lomonosov Moscow State University, Moscow, Russia (email: `rovenska@iiasa.ac.at`)

Tony Q. S. Quek is with the Singapore University of Technology and Design (SUTD), Singapore (email: `tonyquek@sutd.edu.sg`).

The first two authors have equal contributions to this research.

The material in this paper has been presented in part at the 2015 IEEE Conference on Decision and Control [1].

Keywords

multi-agent networks, diffusion process, directed graphs, graph Laplacian, network control, network design

I. Introduction

Large-scale network dynamics received ample research interest over the last decade in the context of group coordination [2], distributed algorithms [3], network control [4], [5], distributed optimization [6], consensus problems [7], [8], and herding and flocking behavior [9]. Network dynamics involve interactions between agents and relate to the diffusion of a continuous quantity within a generic network [10]–[14]. In this work, we establish a probabilistic diffusion framework that describes in continuous time the movement of such a continuous quantity within a multi-agent network. The main contributions of our framework are (i) to present two classes of linear update rules according to the conservation of the network property and characterize the corresponding dynamical network behavior, (ii) to include network control into the framework resulting in the study of the network stability and convergence under different conditions, and (iii) to impose flow modifications by means of network design.

This framework builds on consensus models involving Markovian state transitions [2], [15]–[18], as well as multi-agent gossiping models describing interactions between pairs of agents [14]. We generalize these models and introduce two classes of linear inter-agent update rules depending on whether the total quantity initially present in the network is conserved. This enables our framework to account for a wider range of network phenomena: financial and trade assets, as well as human migration, can be modeled using conservative flows, while opinions follow non-conservative network dynamics. Going beyond symmetric, unweighted graphs [19], we focus on weighted graphs with asymmetric update rules and derive the corresponding differential equation that describes the diffusion of the considered quantity over the network averaged over all sample paths. We highlight the differences in transient and stationary behavior for both update rules, the effects of network asymmetry, and the conditions for convergence in networks with switching topologies.

Building on existing leader-follower models [20], [21], we extend the homogeneous differential equation that describes the diffusion process to its inhomogeneous form. By doing so, we can model the addition and subtraction of the considered quantity to and from the multi-agent network. We show that diffusion processes in the presence of stubborn agents [14], the process of dynamic learning [18], or the PageRank algorithm with damping [22], can be expressed in terms of the inhomogeneous equation. Moreover, these examples illustrate how control actions can result in changes of the rate transition matrix that governs the network dynamics. In addition, we define the constraints on the input vector and network topology under which networks with exogenous excitation remain stable and converge to a steady state. Aside from individual network trajectories, we also provide a method based on the support function of non-empty closed convex sets to define the entire set of attainable network states. Moreover, this method provides insight in the difference between attainability sets of conservative and non-conservative networks based on the Hausdorff distance between these sets.

Our framework enables network control through the introduction of controls at individual nodes or the adjustment of the network structure. Besides imposing external control variables, we address the modification of inter-agent interactions to achieve network control. By modifying the transition rate matrix governing the network dynamics, we shift the eigenvalues of the characteristic modes of the system and modify the dynamics. Furthermore, we present an adaptive heuristic that models the modification of the network structure as a Markov decision process (MDP). Perturbations to the transition rate matrix can be searched efficiently using a reinforcement learning algorithm [23], achieving suboptimal control with quick convergence. In conclusion, the proposed network control and network design processes form a toolbox for the micromanagement of diffusion in networks.

The remainder of the paper is structured as follows. Section II introduces two essential classes of stochastic update rules to model diffusion in networks. Section III discusses the stability and convergence characteristics of conservative and non-conservative networks, while Section IV extends the homogeneous equations to their inhomogeneous forms. Section V discusses network structure modifications for network control and Section VI provides some concluding remarks.

II. Stochastic update rules

We consider a population $\mathcal{V}$ of interacting agents $\mathcal{V}_i$, where $i \in \mathcal{I} = \{1, 2, \ldots, n : n \in \mathbb{Z}^+\}$. These agents have the capacity to handle a continuous quantity or node property $S_i(t) \in \mathbb{R}, t \geq t_0$. All node properties are gathered in the state vector $S(t) = [S_1(t) \ldots S_n(t)]^{\mathrm{T}}$, $S(t) \in \mathbb{R}^n$. Given the initial conditions $S_i(0) = S_{i,0}$, the node properties evolve over time according to a stochastic update process that follows a clock ticking at times determined by a Poisson process. The probabilistic interactions between the agents can be described by a weighted digraph $G = (\mathcal{V}, \vec{\mathcal{E}}, w)$, where $\mathcal{V}$ is the set of agents, $\vec{\mathcal{E}}$ is the set of directed links (i, j) between pairs of agents from $\mathcal{V}$, and the weight function $w\colon \vec{\mathcal{E}} \mapsto \mathbb{R}^+$ captures the update rates and liabilities in the network. The weighted adjacency matrix can be represented as

$$A_G(i,j) = \begin{cases} w(i,j) \text{ if } (i,j) \in \vec{\mathcal{E}}\,, \\ 0 \qquad\quad \text{otherwise} \ . \end{cases} \tag{1}$$

The weighted in-degree and out-degree matrices are diagonal matrices with diagonal elements given by

$$D_G^{(\text{in})}(j,j) = \sum_i A_G(i,j)\,, \tag{2}$$

$$D_G^{(\text{out})}(i,i) = \sum_j A_G(i,j)\,. \tag{3}$$

The exact meaning of the edge weight and the direction of the links will be made explicit when we analyze the update rules, referred to as protocols, in the following Section. Since the interactions between agents can be asymmetric, we will introduce two different Laplacians that refer to the in-degree and the out-degree of each node. We define the weighted in-degree and out-degree Laplacians as

$$L_G^{(\text{in})} = D_G^{(\text{in})} - A_G\,, \tag{4}$$

$$L_G^{(\text{out})} = D_G^{(\text{out})} - A_G\,. \tag{5}$$

Depending on the choice of the stochastic update rule used in the inter-agent probabilistic interactions, we will characterize the flow dynamics of networks operating under different protocols. Here, we describe two main classes of linear update rules that result in linear, time-invariant differential equations in the node property and corresponding matrix differential equations in the diffusion probabilities.[1] These update rules are distinguished by the conservation or the non-conservation of the total property initially present in the network. The networks applying the conservative and non-conservative protocols will be referred to as conservative and non-conservative networks, respectively.

A. *Conservative networks*

We first consider a protocol where the total property in the network is conserved at every instant in time. Conservative updating is relevant for the description of conservative flow dynamics in a network, including the flow of material and physical assets. In this respect, conservative networks

[1]For non-linear update rules, we refer to [24].

are able to represent stylized instances of hydraulic, financial, or trade networks. Here, agents obey the conservative update rule

$$\begin{aligned} S_i(t+\Delta t) &= S_i(t) + C_{ij} S_j(t) \\ S_j(t+\Delta t) &= (1 - C_{ij}) S_j(t)\,, \end{aligned} \tag{P1}$$

where $i, j \in \mathcal{I}$, $(i,j) \in \vec{\mathcal{E}}$. The parameter $C_{ij} \in (0,1]$ is a measure of liability or responsibility of agent j towards agent i, and Δt is an infinitesimal time interval. For every edge $(i,j) \in \vec{\mathcal{E}}$, there exists a clock obeying an independent Poisson process with rate $r_{ij} > 0$. The protocol (P1) is executed for nodes i and j when the independent Poisson clock of (i,j) ticks at time t. The following Lemma characterizes the property dynamics of the instance-averaged value of S in conservative networks.

Lemma 1. *Let $\bar{S}(t)$ denote the expected value of $S(t)$ averaged over all sample paths. The dynamics of the expected property for a network applying* (P1) *are defined by the governing equation*

$$\dot{\bar{S}}(t) = Q \bar{S}(t)\,, \tag{A}$$

where $Q = -L_G^{(\mathrm{in})}$, the weight function is defined as $w(i,j) = C_{ij} r_{ij}$, and

$$Q_{ij} = \begin{cases} C_{ij} r_{ij} & \text{if } i \neq j\,, \\ -\sum_{k \neq i} C_{ki} r_{ki} & \text{if } i = j\,. \end{cases} \tag{6}$$

Proof: We first note that the total update rate for a node $i \in \mathcal{V}$ is given by $r_i = \sum_j r_{ij}$, and that the total update rate of the network is given by $r = \sum_i r_i$. Assume that a global network clock is ticking at rate r. Then, the probability that the clock will activate edge (i,j) is given by r_{ij}/r, where in the limit of large-scale networks $r \approx 1/\Delta t$. Consequently, when updating follows (P1), the probabilistic update of the property of the nodes corresponding to the edge (i,j) is given by

$$\bar{S}_i(t+\Delta t) - \bar{S}_i(t) = \sum_{j \neq i} r_{ij}\, \Delta t\, C_{ij}\, \bar{S}_j(t) \tag{7}$$

$$\bar{S}_j(t+\Delta t) - \bar{S}_j(t) = -\sum_{i \neq j} r_{ij}\, \Delta t\, C_{ij}\, \bar{S}_j(t)\,, \tag{8}$$

which can be succinctly written as

$$\bar{S}_i(t+\Delta t) - \bar{S}_i(t) = \sum_{j \neq i} \Delta t (r_{ij} C_{ij} \bar{S}_j(t) - r_{ji} C_{ji} \bar{S}_i(t))\,. \tag{9}$$

Dividing by Δt and taking the limit for $\Delta t \to 0$, we get a system of differential equations

$$\dot{\bar{S}}(t) = -L_G^{(\mathrm{in})} \bar{S}(t)\,, \tag{10}$$

which concludes the proof. □

Considering (A), we notice that $\bar{S}(t)$ belongs to the class of continuously differentiable functions $\mathcal{C}^1[t_0, \infty)^n$.

Corollary 1. *The matrix $Q = -L_G^{(\mathrm{in})}$ of a conservative network represents the transition rate matrix of a continuous-time Markov chain (CTMC). The transition probabilities $P_{ij}(t)$ of the CTMC are solutions of the differential equation*

$$\dot{P}(t) = QP(t)\,, P(t) = [P_{ij}(t)]\,. \tag{11}$$

Proof: From (6), we notice that

$$Q_{jj} \doteq -\sum_{i \neq j} Q_{ij} \quad \forall\ j \in \mathcal{I}, \tag{12}$$

such that the columns of Q sum to zero. It follows that Q represents the transition rate matrix of a positive recurrent CTMC. Accordingly, the property diffusion can be described by a CTMC whose state space is equivalent to the agent set $\mathcal{V}$ and whose instantaneous state is denoted by $X(t)$. Given that the diffusion dynamics can be described by a CTMC, we can write [25]

$$\Pr[X(t+u) = i] = \sum_j P_{ij}(u) \Pr[X(t) = j] \ \ ,\forall\ \ u \in (0, \infty) \tag{13}$$

for some state $i \in \mathcal{I}$, where

$$P_{ij}(u) = \Pr[X(t+u) = i | X(t) = j] \tag{14}$$

describes the probability that an infinitesimal piece of property is in state i (i.e. agent i) at time $t+u$, given that it was in state j (i.e. agent j) at time t. From (13), it follows that the transition probability matrix $P = [P_{ij}]$ satisfies

$$P(t+u) = P(t)P(u) \quad \forall\ \ t, u \in (0, \infty)\,, \tag{15}$$

or the Chapman-Kolmogorov equation. Assuming that the limits $\lim_{h\to 0} P(h) = P(0)$ and $\lim_{h\to 0} \dot{P}(h) = \dot{P}(0)$ exist, we can then adopt the relation $P(0) = I_n$ where I_n is the identity matrix of dimension n. By taking the limit $u \equiv \Delta t \to 0$ in (15) and using the appropriate Taylor series expansion about $P(0)$, we then obtain the following deterministic differential equation

$$\dot{P}(t) = QP(t) \tag{16}$$

where $Q = \dot{P}(0) = [Q_{ij}]$. □

We can interpret (11) as an equation describing the diffusion of transition probabilities between the various agents over time.

Note that Lemma 1 can also be demonstrated via a probabilistic interpretation of the CTMC. It can be shown that $P(t)$ is continuous in t, $\forall t \geq 0$ [25]. From (12), it follows that the columns of $\dot{P}(t)$ always sum to zero. This shows that for each origin agent j, the sum over all the agents i of the time-cumulative transition probabilities P_{ij} is conserved over time at a value of 1, as expected from conventional laws of probability. We now consider the expected value of $S_i(t)$ averaged over all sample paths, which is given by the column vector

$$\bar{S}(t) = P(t)\bar{S}(0)\,. \tag{17}$$

This illustrates that the sum of $\bar{S}$ over all agents remains a conserved quantity when (P1) is applied. If the system starts from a known, deterministic state, then the bar in $\bar{S}(0)$ can be omitted. We will further indicate $\bar{S}(0)$ by S_0. Combining (11) and (17), we find again (A).

B. Non-conservative networks

We now consider a protocol where property diffuses between agents by means of a convex updating protocol. This protocol is of interest for opinion dynamics [3], [14], or preference dynamics in cultural theory [26]. Here, agents obey the following convex update rule [14]

$$S_i(t + \Delta t) = C_{ij}S_j(t) + (1 - C_{ij})S_i(t)\,, \tag{P2}$$

whenever the Poisson clock ticks for a pair of agents $i, j \in \mathcal{I}$, $(i, j) \in \vec{\mathcal{E}}$. In other words, when the (i, j)-th Poisson clock activates the link between agents i and j, agent i is triggered to poll the property value of agent j with a measure of confidence C_{ij} and update its own value accordingly. The following Lemma characterizes the property dynamics in non-conservative networks.

Lemma 2. *The dynamics of the expected property for a network applying* (P2) *are defined by the governing equation*

$$\dot{\bar{S}}(t) = Q\bar{S}(t)\,, \tag{A}$$

where $Q = -L_G^{(\text{out})}$, $w(i, j) = C_{ij}r_{ij}$, *and*

$$Q_{ij} = \begin{cases} C_{ij}r_{ij} & \text{if } i \neq j\,, \\ -\sum_{k\neq i} C_{ik}r_{ik} & \text{if } i = j\,. \end{cases} \tag{18}$$

Proof: When property updating follows (P2), the probabilistic update of the property of node $\mathcal{V}_i \in \mathcal{V}$ is given by

$$\bar{S}_i(t+\Delta t) - \bar{S}_i(t) = \sum_{j \neq i} (r_{ij}\Delta t) C_{ij} (\bar{S}_j(t) - \bar{S}_i(t)) \,. \tag{19}$$

Dividing by Δt and taking the limit for $\Delta t \to 0$, we obtain the instance-averaged linear differential equations represented by (A) with $Q = -L_G^{(\text{out})}$. □

Note that Lemma 2 extends the basic consensus algorithm where $\dot{\bar{S}}_i(t) = \sum_{j \in \mathcal{N}_i} \big(\bar{S}_j(t) - \bar{S}_i(t)\big)$, with $\mathcal{N}_i$ the neighborhood of i, to asymmetrically weighted updating. The relevance of the asymmetry will be further discussed in Section III.

Corollary 2. *The matrix $Q = -L_G^{(\text{out})}$ of a non-conservative network represents the transition rate matrix of a CTMC, and the transition probabilities of the CTMC are solutions of the following differential equation*

$$\dot{P}(t) = QP(t) \,, \tag{20}$$

Proof: The proof is similar to the proof of Corollary 1, and follows from the fact that

$$Q_{ii} \doteq -\sum_{j \neq i} Q_{ij} \quad \forall \; i \in \mathcal{I} \,, \tag{21}$$

meaning that the rows of Q all sum to zero. □

The CTMC corresponding to Q represents a random walk on G. In comparison with the transfer of an infinitesimal piece of property in a conservative network, P_{ij} in non-conservative networks represents the probability that node i polls node j to update its own value using the weight C_{ij}. Here, the rows of $\dot{P}(t)$ always sum to zero, and consequently the rows of $P(t)$ always sum to one. This shows that every polling tag originating from an agent i must either still be under the possession of agent i or of some other agent j in the network.

Remark 1. *Lemmas 1 and 2 explicitly link the protocols* (P1) *and* (P2) *to the transition rate matrices. Consequently, the transition rate matrix captures all relevant properties of diffusion over networks, i.e., the update protocol, the network topology, the inter-agent measures of liability/confidence, and the update rates. In the case of a symmetric Q matrix, the in-degree and out-degree Laplacians are identical. Hence, the two protocols are equivalent for symmetric matrices. For asymmetric matrices,* (4) *and* (5) *show that the conservative Q and the transpose of the non-conservative Q are identical if the two corresponding digraphs have the same network topology with equal weights, but with all link directions reversed.*

III. UNCONTROLLED NETWORK DYNAMICS

In this section, we analyze the transient and steady-state characteristics of (A) based on the eigendecomposition of Q. Formulas (11) and (20) can be solved as $P(t) = \exp(Qt)$. Due to the construction of Q as a Laplacian matrix, Q always has the eigenvalue $q_{\mathrm{s}} = 0$. Moreover, since all non-diagonal elements are non-negative, Q is a Metzler matrix for which $\exp(Qt)$ is non-negative for $t \geq 0$. If Q is diagonalizable, then the solution to (A) can be written as

$$\begin{aligned}\bar{S}(t) &= \exp\left(A\Lambda A^{-1}t\right) S_0 \\ &= A\,\mathrm{diag}\left(\exp(q_k t)\right) A^{-1} S_0\,,\end{aligned} \tag{22}$$

where A contains the unit right eigenvectors of Q as columns, A^{-1} contains the corresponding left eigenvectors of Q as rows, q_k represents the eigenvalues of Q, and $\Lambda = \mathrm{diag}(q_k)$. Also,

$$\begin{aligned}\bar{S}(t) &= \sum_k \exp(q_k t) v_{\mathrm{R},k} v_{\mathrm{L}^*,k}^{\mathrm{T}} S_0 \\ &= \sum_k c_k \exp(q_k t) v_{\mathrm{R},k}\,,\end{aligned} \tag{23}$$

where $v_{\mathrm{R},k}$ and $v_{\mathrm{L}^*,k}$ are the unit right and corresponding left eigenvectors[2] of Q in column form, and $c_k = v_{\mathrm{L}^*,k}^T S_0$ are scalars. We notice from (23) that the eigenvalues and eigenvectors reflect the characteristic growth and decay rates of the system, as well as the dominant and weak nodes in the network. Concerning the eigenvalues of Q, Geršgorin's circle theorem states that all eigenvalues of Q reside in the complex plane within the union of the disks $D_i = \{z \in \mathbb{C} : |z - Q_{ii}| \leq \sum_{j \neq i} |Q_{ij}|\}$, $i \in \mathcal{I}$. According to this theorem, Q matrices constructed in compliance with (P1) or (P2) have nonpositive eigenvalues including zero, such that the node quantities are stable and converge to a steady state in finite time. The stationary network state is given by

$$\lim_{t \to \infty} \bar{S}(t) = c_{\mathrm{s}} v_{\mathrm{R,s}}\,, \tag{24}$$

where c_{s} and $v_{\mathrm{R,s}}$ are the scalar and unit right eigenvector corresponding to $q_{\mathrm{s}} = 0$. We now illustrate the dynamics for different strongly connected network classes using the network presented in Fig. 1.

A. *Conservative asymmetric networks*

For conservative networks, we formulate the following Lemma for the stationary behavior.

[2]The left eigenvectors $v_{\mathrm{L}^*,k}$ are only unit in the case where Q is symmetric.

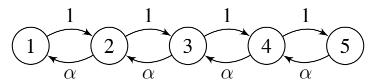

Fig. 1: Path graph P_5 with asymmetric link weights used to illustrate the transient and steady-state behaviors of the various update rules.

Lemma 3. *The stationary value of a strongly connected asymmetric network applying* (P1) *is given by* $v_{\mathrm{R,s}}$ *scaled by* $c_{\mathrm{s}} = \sum_i S_{0,i}/\Psi$ *where* Ψ *is the sum of the entries of* $v_{\mathrm{R,s}}$.

Proof: Here, the column-sum of $Q = -L_G^{(\mathrm{in})}$ is zero, so Q has a unit steady-state left eigenvector $v_{\mathrm{L,s}}$ with equal components. In an asymmetric network, the stationary node values are imbalanced due to the unequal components in $v_{\mathrm{R,s}}$. Considering (23), the proof is concluded. □

When asymmetric liabilities between nodes occur, the stationary distribution will favor attractive over repulsive nodes, and uniform spreading does not occur as a consequence of the conservation of total property. We illustrate this finding for the network depicted in Fig. 1 with $\alpha = 0.2$, and we present in Fig. 2 the evolution of $\bar{S}_i(t)$ over time. In the latter plot, we generate $\bar{S}_i(t)$ by empirically generating sample paths based on the update rule (P1), and analytically determining the expected property from (23).

B. Non-conservative asymmetric networks

For networks that apply the convex update rule (P2), we formulate the following Lemma for the stationary behavior.

Lemma 4. *A strongly connected asymmetric network following the convex update rule* (P2) *always achieves consensus. The consensus value* $c_{\mathrm{v}} = c_{\mathrm{s}}/\sqrt{n}$ *in the infinite time horizon is the following weighted average of* S_0

$$c_{\mathrm{v}} = \frac{1}{\Omega} v_{\mathrm{L,s}}^{\mathrm{T}} S_0 \,, \tag{25}$$

where Ω *is the sum of the entries in* $v_{\mathrm{L,s}}$.

Proof: Since the row-sum of $Q = -L_G^{(\mathrm{out})}$ is zero, $v_{\mathrm{R,s}}$ has equal components. Hence, strongly connected networks with asymmetric updating always achieve agreement. Determining the consensus value requires finding the row of A^{-1} corresponding to $q_{\mathrm{s}} = 0$. For an asymmetric matrix, this corresponds to $v_{\mathrm{L,s}}$ scaled by the factor $\sqrt{n}/\Omega$, since the dot product of this scaled

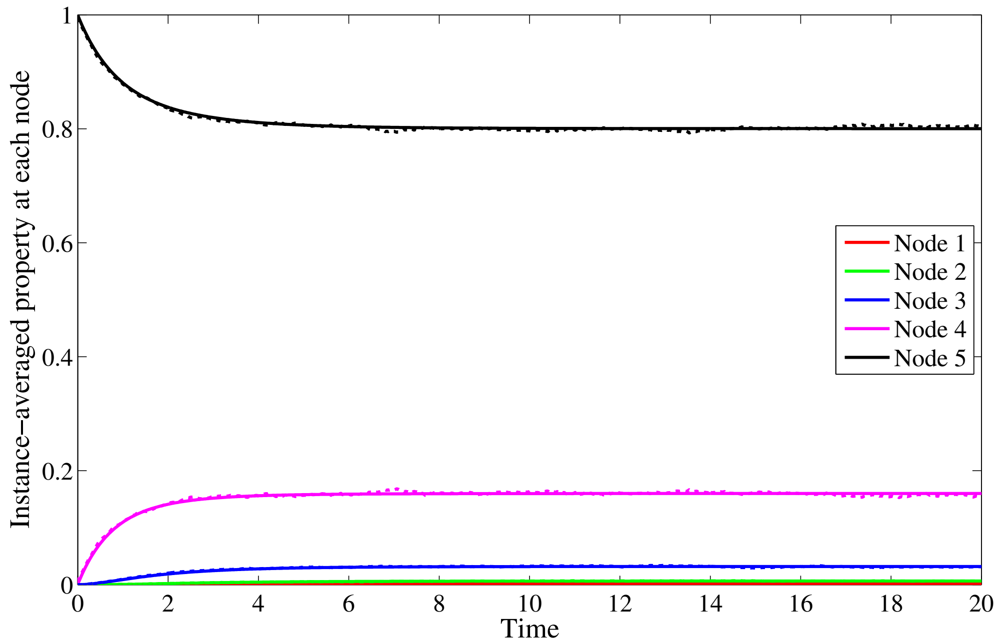

Fig. 2: Comparison of instance-averaged node property obtained through Monte Carlo simulations (dotted lines) and expected property obtained by eigendecomposition of the matrix Q (solid lines) for the asymmetric network in Fig. 1 with $\alpha = 0.2$ under (P1). For the simulations, 5000 trials were performed, and each timestep was discretized into 1000 sub-units. In both cases, the initial conditions were adopted with $S_0 = [0\,0\,0\,0\,1]$.

vector and $v_{\mathrm{R,s}}$ must equal 1 based on the initial conditions $P(0) = I_n = A^{-1}A$. The result is then scaled by the magnitude of the entries of $v_{\mathrm{R,s}}$ to obtain c_{v}. □

We illustrate in Fig. 3 the consensus behavior for the network depicted in Fig. 1 with $\alpha = 0.2$. Here, c_{v} is heavily weighted towards node 5, whose inward link weight exceeds its outward link weight. This means that node 5 is heavily polled by its neighbors. Such a trend is reminiscent of the availability heuristic, where subjects that are encountered or recalled more often are given more thought and emphasis [27].

C. Symmetric networks

In a strongly connected symmetric network, the steady-state right eigenvector has components of equal magnitude in all dimensions regardless of the update rule. We can interpret this as an equal sharing of resources in conservative networks, and as consensus among all agents at a value corresponding to the average of the initial conditions at all the nodes in non-conservative networks [14], [16]–[18]. We illustrate this conclusion by observing $\bar{S}_i(t)$ over time in Fig. 4 for the network depicted in Fig. 1 with $\alpha = 1$. In Fig. 4, we generate $\bar{S}_i(t)$ by both empirically generating sample paths based on the update rules (P1) and (P2), which are equivalent in this

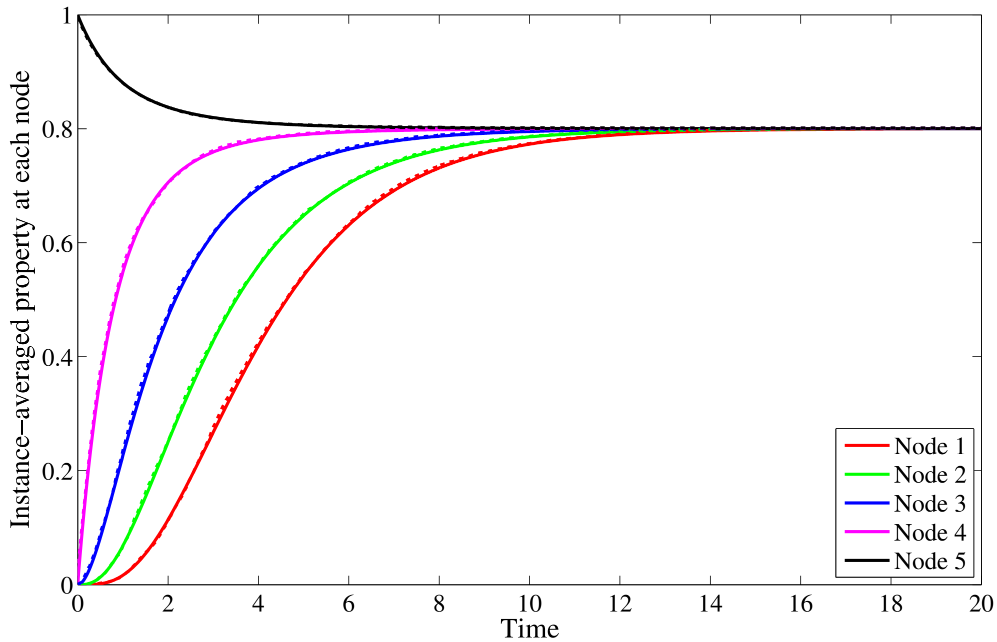

Fig. 3: Comparison of instance-averaged property obtained numerically (dotted lines) and analytically (solid lines) for the asymmetric network in Fig. 1 with $\alpha = 0.2$ under (P2). The simulation parameters are identical to those in Fig. 2. In this case, the unit steady-state left eigenvector is $[0.0016\,0.0078\,0.0392\,0.1960\,0.9798]$ and the unit steady-state right eigenvector is $\frac{1}{\sqrt{5}}[1\,1\,1\,1\,1]$, which gives us $\Omega = 1.2244$ and the corresponding consensus value $c_{\mathrm{v}} = 0.8003$.

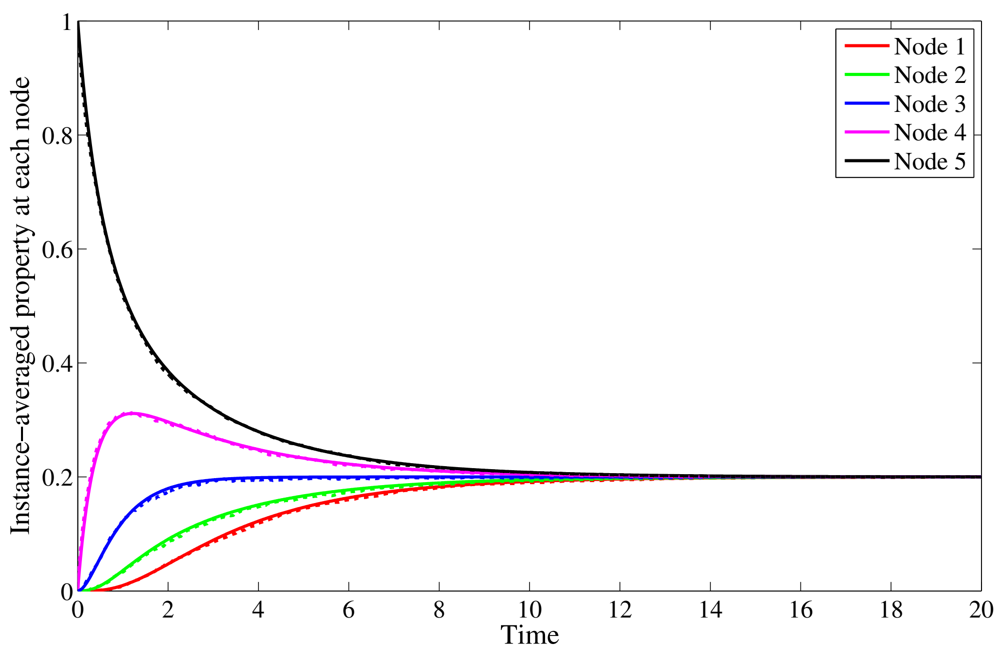

Fig. 4: Comparison of instance-averaged property obtained numerically (dotted lines) and analytically (solid lines) for the symmetric network in Fig. 1 with $\alpha = 1$. The simulation parameters are identical to those in Fig. 2.

case, and analytically determining the expected property from (23).

D. Switching topologies

There are many important scenarios where the network topology can change over time. As an example, connections in wireless sensor networks can be established and broken due to mobility. In this Section, we study the steady-state behavior of networks with switching topologies and provide a condition that leads to convergence under dynamic topologies. Networks with switching topologies converge if they exhibit the same invariant stationary value as defined in Lemma 3 and Lemma 4, which depend on $v_{\mathrm{R},s}$ and $v_{\mathrm{L},s}$ for (P1) and (P2) respectively.

We introduce now two classes of strongly connected, directed graphs for which the weighted Laplacian shares the left or the right eigenvector corresponding to $q_{\mathrm{s}} = 0$. For conservative and non-conservative networks, we have respectively

$$\begin{aligned} \mathcal{G}_{v_{\mathrm{s}}}^{(\mathrm{P1})} &= \{G(\mathcal{V}, \vec{\mathcal{E}}, w) \,:\, \operatorname{rank} L_G^{(\mathrm{in})} = n-1, L_G^{(\mathrm{in})} \times v_{\mathrm{R,s}} = \vec{0}\} \\ \mathcal{G}_{v_{\mathrm{s}}}^{(\mathrm{P2})} &= \{G(\mathcal{V}, \vec{\mathcal{E}}, w) \,:\, \operatorname{rank} L_G^{(\mathrm{out})} = n-1, v_{\mathrm{L,s}} \times L_G^{(\mathrm{out})} = \vec{0}^{\mathrm{T}}\}\,. \end{aligned} \tag{26}$$

Correspondingly, we define the following sets of matrices with equal steady-state eigenvectors as follows

$$\begin{aligned} M_{v_{\mathrm{s}}}^{(\mathrm{P1})} &= \{Q \colon Q = -L_G^{(\mathrm{in})}, Q \times v_{\mathrm{R,s}} = \vec{0}\} \\ M_{v_{\mathrm{s}}}^{(\mathrm{P2})} &= \{Q \colon Q = -L_G^{(\mathrm{out})}, v_{\mathrm{L,s}} \times Q = \vec{0}^{\mathrm{T}}\}\,. \end{aligned} \tag{27}$$

For these network classes, the system dynamics are

$$\dot{\bar{S}}(t) = Q_k \bar{S}(t)\,, \tag{28}$$

where $Q_k \in M_{v_{\mathrm{s}}}^{(\mathrm{P1})}$ when (P1) is applied, and $Q_k \in M_{v_{\mathrm{s}}}^{(\mathrm{P2})}$ when (P2) is applied. The index k changes over time according to $k = f(t)$, $f \colon \mathbb{R}^+ \to \mathcal{I}_M$, where $\mathcal{I}_M$ is the index set of the corresponding set of matrices.

Lemma 5. *Networks obeying* (28) *that are strongly connected and follow* (P1) *or* (P2) *are globally asymptotically convergent if Q_k belongs to $M_{v_s}^{(\mathrm{P1})}$ or $M_{v_s}^{(\mathrm{P2})}$, respectively.*

Proof: The proof follows from the fact that all networks that belong to $M_{v_{\mathrm{s}}}^{(\mathrm{P1})}$ or $M_{v_{\mathrm{s}}}^{(\mathrm{P2})}$ converge to the same invariant quantity, as they share the same right and left eigenvector, respectively. As all elements of $M_{v_{\mathrm{s}}}^{(\mathrm{P1})}$ and $M_{v_{\mathrm{s}}}^{(\mathrm{P2})}$ are globally asymptotically stable, this concludes the proof. □

We introduce now the distance vector $\delta = \bar{S}(t) - c_{\mathrm{s}} v_{\mathrm{R,s}}$. As $c_{\mathrm{s}} v_{\mathrm{R,s}}$ is an equilibrium of the system, we can write

$$\dot{\delta}(t) = Q_k \delta(t)\,. \tag{29}$$

We cannot make a general statement about the definiteness of asymmetric matrices with non-positive eigenvalues. For the matrices in $M_{v_s}^{(\mathrm{P1})}$ or $M_{v_s}^{(\mathrm{P2})}$ that are negative definite, we can bound the convergence speed of the distance vector as follows.

Corollary 3. *Consider a strongly connected graph for which the weighted in-degree or out-degree Laplacian is negative definite. For these networks, δ globally asymptotically converges to zero and the convergence speed can be bounded as*

$$\|\delta(t)\|_2 \leq \|\delta(0)\|_2 \exp(q_{\max} t) \tag{30}$$

where $q_{\max} = \max q_2(M_{v_s}^{(\mathrm{P1})})$ for conservative networks and $q_{\max} = \max q_2(M_{v_s}^{(\mathrm{P2})})$ for non-conservative networks. Here, q_2 is the non-zero eigenvalue with the smallest absolute value of the corresponding transition rate matrix.

Proof: Consider the Lyapunov function $V(\delta) = 1/2\left(\delta(t)^T\delta(t)\right)$. The first derivative can be written as

$$\dot{V}(\delta(t)) = 1/2\left(\delta(t)^{\mathrm{T}} Q_k^{\mathrm{T}} \delta(t) + \delta(t)^{\mathrm{T}} Q_k \delta(t)\right) , \tag{31}$$

so $\dot{V}(\delta(t)) \leq 0$. Using the Courant-Fischer theorem, and similar to [16], the proof is concluded. □

Remark 2. *A relevant question is if it is possible to verify if two matrices Q_1 and Q_2 belong to the same set $M_{v_s}^{(x)}$, $x \in \{P1, P2\}$. The common eigenvector problem can be solved when the eigenvalue is not known [28]. For the special case where the common eigenvalue is equal to zero, two matrices Q_1 and Q_2 have the same eigenvector corresponding to $q_s = 0$ if*

$$\mathrm{null}(Q_1) = \mathrm{null}(Q_2) \,. \tag{32}$$

IV. NETWORK CONTROL BY EXOGENOUS EXCITATION

To model the exogenous addition and subtraction of property to multi-agent networks, we extend the homogeneous equation (A) to include an inhomogeneous term

$$\dot{\bar{S}}(t) = Q\bar{S}(t) + U(t) \,. \tag{B}$$

The input vector $U(t)$ belongs to the set of admissible controls $\mathcal{U} = \{U \in \mathbb{R}^n \,|\, U(t) \in \hat{\mathcal{C}}[t_0, \infty)^n\}$, where $\hat{\mathcal{C}}$ represents the class of piecewise continuous functions. Since (B) is linear in $U(t)$, $U(t)$ can either be the same over all sample paths or averaged over all sample paths. For time-invariant matrix Q, the solution to (B) is the Carathéodory solution

$$\bar{S}(t) = \bar{S}_{\mathrm{h}}(t) + \int_0^t \exp(Q(t-\tau))U(\tau)d\tau\,, \tag{33}$$

where $\bar{S}_{\mathrm{h}}(t) = \exp(Qt)S_0$. This can be interpreted as the sum of the solution to the homogeneous equation (A) and the convolution of the input $U(t)$ with the impulse response to (B) for every node. The state variables considered in conservative and non-conservative networks take values over $\mathbb{R}^+$. In fact, we can show that independently of the initial conditions, the positivity of the network properties is guaranteed. Positive systems are of particular importance since they often arise in practical situations, such as in transport networks, storage systems, and stochastic models where the state variables and probabilities take non-negative values.

Definition 1. *The linear system* (B) *is said to be positive if and only if for every non-negative initial state* S_0 *and every non-negative input* $U(t)$*,* $\bar{S}(t)$ *is non-negative [29].*

In other words, if a linear system is positive, then $\mathbb{R}^n_+$ is a positive invariant set.

Lemma 6. *The linear system represented in* (B) *is a positive linear system.*

Proof: By construction, the system matrix Q is a Metzler matrix, i.e., $Q_{ij} \geq 0, i \neq j$. When the system matrix is a Metzler matrix, the positivity of the system (sufficiency and necessity) can be proved based on the direction of $\dot{\bar{S}}(t)$ toward the interior of $\mathbb{R}^n_+$ when $\bar{S}(t)$ is on the boundary of $\mathbb{R}^n_+$ [29]. □

In the following subsections, we first present practical use cases where the network dynamics can be expressed by the inhomogeneous equation (B) with constant and time-varying control variable U. Interestingly, the use cases with stubborn agents [14] and dynamic learning [18] illustrate that network control can result in modifications of the system matrix and in some cases in a non-singular Q. This motivates the study of stability and convergence in the presence of exogenous inputs for singular and non-singular system matrices. Finally, we present a methodology based on the support function to characterize the attainability sets at a given time t for networks with exogenous control. Moreover, we compare the attainability sets of conservative and non-conservative networks in terms of the Hausdorff distance.

A. Network dynamics with static inputs

For conservative networks, a popular example is the discrete-time damped PageRank algorithm [22], [30]. PageRank is a link analysis tool for a network of hyperlinked webpages, able to rank their relative importance. The algorithm describes the diffusion of a conserved amount of scores $S_i(t)$, and can be formulated equivalently as the following continuous-time model with constant U

$$\dot{\bar{S}}(t) = \alpha Q \bar{S}(t) + \frac{1-\alpha}{n}\bar{1}\,, \tag{34}$$

where Q is the negative of the weighted in-degree Laplacian as defined in (6), and $\alpha \in [0,1]$ represents a damping factor that captures typical internet user behavior. Here, $\bar{1}$ denotes the all-one vector. In this example for controlled conservative networks, the transition rate matrix Q is a singular matrix.

We present now an example of controlled network dynamics where the transition rate matrix is modified and in general non-singular. Adopting the definition proposed in [14], as well as the non-conservative update rule (P2), an agent is called stubborn if it does not adjust its own value based on the values of neighboring nodes. This scenario is of interest to model opinion dynamics where a set of agents has constant opinion. In these networks, the out-degree of a stubborn agent is zero and the corresponding row of Q is a zero-row.[3] For example, in the presence of two stubborn agents $a_1 = 2$ and $a_2 = n$, the governing equation can be written as

$$\begin{bmatrix} \dot{\bar{S}}_1 \\ \vdots \\ \dot{\bar{S}}_n \end{bmatrix} = \begin{bmatrix} Q_{1,1} & Q_{1,2} & \cdots & Q_{1,n} \\ 0 & 0 & \cdots & 0 \\ Q_{3,1} & Q_{3,2} & \cdots & Q_{3,n} \\ \vdots & \vdots & \ddots & \vdots \\ 0 & 0 & \cdots & 0 \end{bmatrix} \begin{bmatrix} \bar{S}_1 \\ \vdots \\ \bar{S}_n \end{bmatrix}, \tag{35}$$

which can be reformulated as

$$\begin{bmatrix} \dot{\bar{S}}'_1 \\ \vdots \\ \dot{\bar{S}}'_{n-2} \end{bmatrix} = \begin{bmatrix} Q'_{1,1} & Q'_{1,2} & \cdots & Q'_{1,n-2} \\ \vdots & \vdots & \ddots & \vdots \\ Q'_{n-2,1} & Q'_{n-2,2} & \cdots & Q'_{n-2,n-2} \end{bmatrix} \begin{bmatrix} \bar{S}'_1 \\ \vdots \\ \bar{S}'_{n-2} \end{bmatrix} + \begin{bmatrix} \vdots & \vdots \\ B_{k,a_1} & B_{k,a_2} \\ \vdots & \vdots \end{bmatrix} \begin{bmatrix} \bar{S}_{a_1} \\ \bar{S}_{a_2} \end{bmatrix}, \tag{36}$$

[3]Conversely, if the in-degree of an agent equals zero, the node acts as a sink, which can receive property from every neighbor but does not contribute to its neighborhood. This case, where Q contains a zero column, does not lead to a convenient reduction of the state space.

where B_{k,a_1} and B_{k,a_2} are the a_1-th and a_2-th columns of Q with the a_1-th and a_2-th entries omitted. This gives us

$$\dot{\bar{S}}'(t) = Q'\bar{S}'(t) + BU_{\mathrm{st}}\,, \tag{37}$$

where $\bar{S}'$ and Q' represent the reduced state space and reduced transition rate matrix, and $U_{\mathrm{st}} = [\bar{S}_{a_1} \cdots \bar{S}_{a_n}]^T$ contains the static quantities of the stubborn agents. From (37), we notice that stubborn agents allow for a reduction of the state space and a formulation equivalent to (B) with constant but possibly different inputs for different stubborn nodes and $U = BU_{\mathrm{st}}$. The reduced state space excludes the stubborn agents and the reduced transition rate matrix excludes the rows and columns corresponding to these agents. The formulation with reduced state space corresponds to an open-loop control system.

Since U is constant, it is known that bounded-input bounded-output (BIBO) stability of (37) is guaranteed iff all eigenvalues of Q' have negative real components. In other words, a finite input to the system always leads to a finite output. Since Q' is constructed differently from Q, the spectrum of homogeneous and inhomogeneous systems is not identical. Define $\mathcal{I}_{\mathrm{st}} = \{i \,|\, \bar{S}_i(t) \,\text{is constant}\}$ as the index set of stubborn agents. Then, we can write $Q_{ii} = -\sum_{j\neq i, j\notin\mathcal{I}_{\mathrm{st}}} Q_{ij} - \sum_{j\neq i, j\in\mathcal{I}_{\mathrm{st}}} Q_{ij}$, and the row sum of Q' satisfies

$$Q'_{ii} + \sum_{j\neq i} Q'_{ij} \leq 0\,. \tag{38}$$

Thus, Q' does not have a zero eigenvalue in general and is non-singular in general. In the following Lemma, we provide a condition that guarantees the non-singularity of Q'.

Lemma 7. *In a network with stubborn agents, the transition rate matrix Q' of the reduced state space is non-singular if all nodes are connected to at least one stubborn agent.*

Proof: If each agent is connected to at least one stubborn agent, Q' is strictly diagonally dominant and we can write

$$Q'_{ii} + \sum_{j\neq i} Q'_{ij} < 0\,. \tag{39}$$

According to Geršgorin's circle theorem, all eigenvalues of Q' reside in the complex plane within the union of the disks $D_i = \{z \in \mathbb{C} \,:\, |z - Q'_{ii}| \leq \sum_{j\neq i} |Q'_{ij}|\}\,,\ 1 \leq i \leq n'$ with n' the dimension of Q'. As $|Q'_{ii}| > \sum_{j\neq i} |Q'_{ij}|$ for a strictly diagonally dominant matrix, $\mathcal{Q}'$ cannot have a zero eigenvalue and is invertible. □

Lemma 7 shows that the eigenvalues of networks with stubborn agents are on average more concentrated around Q'_{ii}, which can accelerate the network dynamics.

B. Network dynamics with dynamic inputs

We present here an example of controlled network dynamics with dynamic inputs, where the transition rate matrix is modified due to closed-loop control actions. In dynamic learning, each node updates its own value based on the values of its neighboring nodes, as well as the difference of its own value with a measurement of the system state[4] [18]. This scenario is of interest to model tracking systems that are augmented with the information present in the neighborhood of each node. The dynamics of an individual node can be represented by the following update rule

$$S_i(t+\Delta t) = S_i(t) + \sum_{j\neq i} C_{ij}(S_j(t) - S_i(t)) + \beta(D_i(t) - S_i(t))\,, \tag{40}$$

where $D_i(t)$ represents the measurement of node i at time t. If the measurements of all nodes are made at a rate ρ, then the corresponding governing equation is

$$\dot{\bar{S}}(t) = (Q - \beta' I_n)\bar{S}(t) + \beta' D(t)\,, \tag{41}$$

where $\beta' = \beta\rho$, and where $r_{ij} = \rho$ in the construction of Q_{ij}. This is again reminiscent of (B) with time-varying input vector $U = \beta' D(t)$, and corresponds to closed-loop proportional control systems with reference input $D(t)$ and proportional gain β'. For constant β', iff all eigenvalues of $Q_D = Q - \beta' I_n$ have negative real components, then an input $\beta' D(t)$ that is bounded for all time $t > 0$ will result in BIBO stability. Note that if Q corresponds to a CTMC and $\beta' > 0$, then the eigenvalues of Q_D are exactly β' less than the eigenvalues of Q, and the resultant system is guaranteed to be BIBO stable, provided β' takes the same value for all agents.

C. Convergence and stability for controlled network dynamics

In this section, we analyze the convergence behavior of the inhomogeneous equation (B) both for singular and non-singular transition rate matrices. The solution to the inhomogeneous equation is given in (33) for an input vector $U(t) \in \mathcal{U}$. It is relevant to study the special case of constant input vectors, for instance when the input vectors belong to the boundary of admissible set $\partial\mathcal{U}$. For constant input vectors, the solution to (B) is given by

$$\begin{aligned}
\bar{S}(t) &= A\exp(t\Lambda)A^{-1}S_0 + \int_0^t A\exp((t-\tau)\Lambda)A^{-1}U\mathrm{d}\tau \\
&= \sum_k c_k \exp(q_k t) v_{\mathrm{R},k} + \sum_k \int_0^t \exp(q_k(t-\tau)) v_{\mathrm{R},k} v_{\mathrm{L}^*,k}^T U \mathrm{d}\tau \\
&= \sum_k c_k \exp(q_k t) v_{\mathrm{R},k} + \sum_k u_k \int_t^0 \exp(q_k(t-\tau))\mathrm{d}(t-\tau) v_{\mathrm{R},k}\,,
\end{aligned} \tag{42}$$

[4] All these are performed simultaneously, in contrast to (P2).

where $u_k = v_{\mathrm{L}^*,k}^T U$. This result can be further developed for non-singular and singular transition rate matrix.

Non-singular Q: As Q has no zero eigenvalues, (42) can be written as

$$\bar{S}(t) = \sum_k c_k \exp(q_k t) v_{\mathrm{R},k} + \sum_k u_k q_k^{-1} (\exp(q_k t) - 1) v_{\mathrm{R},k} \,, \tag{43}$$

and the steady-state behavior is given by

$$\lim_{t\to\infty} \bar{S}(t) = S^* = c_\mathrm{s} v_{\mathrm{R,s}} - \sum_k u_k q_k^{-1} v_{\mathrm{R},k} \,. \tag{44}$$

Alternatively, the steady state can also be found by means of the inverse of Q as follows

$$S^* = -Q^{-1} U \,. \tag{45}$$

Both formulations allow us to define the set of attainable stationary network states $\mathcal{S}(\infty) \subset \mathbb{R}^n$ as a function of the set of admissible controls $\mathcal{U}$.

Singular Q: When Q is singular with single zero eigenvalue, we get

$$\begin{aligned}\bar{S}(t) =& \sum_k c_k \exp(q_k t) v_{\mathrm{R},k} \\ &+ \sum_{k\neq 1} u_k q_k^{-1} (\exp(q_k t) - 1) v_{\mathrm{R},k} + u_\mathrm{s} t v_{\mathrm{R,s}} \,,\end{aligned} \tag{46}$$

with u_s and $v_{\mathrm{R,s}}$ the scalar and eigenvector corresponding to $q_\mathrm{s} = 0$. By taking the limit over time, we get

$$\lim_{t\to\infty} \bar{S}(t) = c_\mathrm{s} v_{\mathrm{R,s}} - \sum_{k\neq 1} u_k q_k^{-1} v_{\mathrm{R},k} + \lim_{t\to\infty} u_\mathrm{s} t v_{\mathrm{R,s}} \,. \tag{47}$$

Since u_s only equals zero for $U = 0$, (47) illustrates that the stationary network state under constant input U is unbounded both for conservative and non-conservative networks.

Remark 3. *In Section III, we demonstrated that the stationary behavior of uncontrolled networks only depends on the left and right eigenvector of Q corresponding to $q_\mathrm{s} = 0$. As opposed to these results, the stationary behavior of networks under control is a function of all eigenvectors of Q, which can be observed in* (44) *and* (47)*. Therefore, while the uncontrolled non-conservative dynamics always led to consensus, this is not the case anymore for controlled non-conservative networks. The set of attainable network states in steady state for uncontrolled non-conservative networks is represented by a point in $\mathbb{R}_+^n$, while the set of attainable network states for controlled non-conservative networks does not have this restriction. In fact, we observe that the presence of stubborn agents in the network results in polarization of the opinions in steady state.*

We illustrate the former results by revisiting the use case of the stubborn agents presented in Section IV-A. Without stubborn agents, Q has by construction eigenvalue $q_{\mathrm{s}} = 0$ and is singular, in which case we observe from (47) that BIBO stability is no longer guaranteed and the system is instead only marginally stable. For the convergence and stability of the system with reduced state space, we formulate the following Lemma.

Lemma 8. *If each agent is connected to at least one stubborn agent, then the network state converges to* $\bar{S}'^{*} = -Q'^{-1}BU_{\mathrm{st}}$*, with* B *and* U_{st} *defined in* (35)*. Moreover, the equilibrium is globally asymptotically stable.*

Proof: Building on Lemma 7, the poles of Q' lie in the open left half-plane and Q' is non-singular. Therefore, the first assertion follows from the steady state behavior expressed in (44) and (45). We express the system dynamics of the inhomogeneous equation as a homogeneous equation in the deviation of the network state from steady state $\bar{S}'_{\Delta}(t) = \bar{S}' - \bar{S}'^{*}$. To prove the global asymptotic stability, we distinguish between symmetric and asymmetric matrices Q'. For the symmetric case, the Lyapunov function $V = \bar{S}'^{T}_{\Delta}\bar{S}'_{\Delta}$ can be used and we obtain

$$\dot{V} = \bar{S}'^{\mathrm{T}}_{\Delta} Q'^{\mathrm{T}} \bar{S}'_{\Delta} + \bar{S}'^{\mathrm{T}}_{\Delta} Q' \bar{S}'_{\Delta} < 0 \ \ , \ \ \forall \ \bar{S}'_{\Delta} \neq \bar{0} \tag{48}$$

since Q' and thus its transpose are negative definite, due to Lemma 7. This demonstrates that the equilibrium point of the network is globally asymptotically stable, and the location of the point can be obtained by setting $\dot{\bar{S}}'_{\Delta} = \bar{0}$. The Lyapunov function above does not hold for nonsymmetric Q'. However, because Q' is strictly diagonally dominant, the existence of a Lyapunov function for Q' can be demonstrated [31]. One such Lyapunov function is $V = \max_i |\bar{S}'_{\Delta,i}|$, which proves the global asymptotic stability of $\bar{S}'$ for asymmetric Q'. □

D. Set of attainability: analysis and comparison

It is very instructive to study the set of attainability, which is the set of states that can be reached by using all possible controls. The set of attainability for conservative and non-conservative networks can be expressed as

$$\begin{aligned} \mathcal{S}(t) \equiv \mathcal{S}(t_0, t, \mathcal{M}_0) = \{S(t) \in \mathbb{R}^n \mid S(t) = e^{(t-t_0)Q} S_0 \\ + \int_{t_0}^{t} e^{(t-\tau)Q} U(\tau) \mathrm{d}\tau, S_0 \in \mathcal{M}_0, U(\tau) \in \mathcal{U}\}\,, \end{aligned} \tag{49}$$

where $\mathcal{M}_0$ is the set of possible initial values S_0 and $\mathcal{U}$ is the compact set of admissible controls in $\mathbb{R}^n$.[5] In view of conservative and non-conservative networks, we aim to describe the differences between the corresponding attainability sets at a given time t when the dynamics take place over the same network. To avoid confusion, we will indicate the system matrices for the conservative and non-conservative network dynamics by $Q_{\rm c}$ and $Q_{\rm nc}$ respectively. When the network structure is the same, $Q_{\rm c}$ differs from $Q_{\rm nc}$ only on the diagonal. Different methods exist to describe the attainability set, for instance by using the maximal principle [32] or by means of ellipsoidal methods that allow to numerically calculate approximations of the attainability set in terms of inner and outer bounds [33]. Here, for the characterization of attainability sets we propose to make use of the support function, which is widely applied in the analysis of convex sets [34]. The set of attainability can be written also by means of the Minkowski sum

$$\mathcal{S}(t) = e^{(t-t_0)Q}\mathcal{M}_0 + \int_{t_0}^{t} e^{(t-\tau)Q}\mathcal{U}\mathrm{d}\tau \,. \tag{50}$$

The Minkowski sum and the linear transformations in (50) preserve compactness and convexity [34]. Therefore, if the initial set $\mathcal{M}_0$ and set of admissible controls $\mathcal{U}$ are compact and convex, then the set of attainability $\mathcal{S}(t)$ is also compact and convex. Every non-empty compact convex set $\mathcal{F}$ is uniquely determined by its support function $c(\mathcal{F},\psi)$, which is defined as

$$c(\mathcal{F},\psi) = \sup_{f\in\mathcal{F}}\langle f,\psi\rangle \,, \tag{51}$$

where $\langle .,. \rangle$ represents the inner product on $\mathbb{R}^n$. For $\psi \in \mathcal{S}_n(0,1) = \{x \,|\, \|x\| = 1\}$ and $\|\cdot\|$ the ℓ^2-norm, the support function represents the signed distance between the origin and the hyperplane $\Gamma_\psi = \{x \,|\, \langle x,\psi\rangle = c(\mathcal{F},\psi)\}$. If $c(\mathcal{F}_1,\psi) = c(\mathcal{F}_2,\psi)\,, \forall\psi \in \mathbb{R}^n$, then $\mathcal{F}_1 = \mathcal{F}_2$. Since $c(\mathcal{F},k\psi) = k\cdot c(\mathcal{F},\psi)\,,\, \forall k \geq 0$, the support function can be used with a restriction of ψ to the unit sphere $\mathcal{S}_n(0,1)$. We propose to use the Hausdorff metric to measure the distance between the attainability sets of the conservative and non-conservative networks at a given time t. The Hausdorff distance is a metric that describes the distance between subsets in a metric space and is defined as

$$h(\mathcal{F}_1,\mathcal{F}_2) = \min_{r\geq 0}\left\{r \,|\, \mathcal{F}_1 \subset \mathcal{F}_2 + \mathcal{B}_n(0,r), \mathcal{F}_2 \subset \mathcal{F}_1 + \mathcal{B}_n(0,r)\right\} \,, \tag{52}$$

where the n-dimensional ball around the origin with radius r is represented by $\mathcal{B}_n(0,r) = \{x \,|\, \|x\| \leq r\}$. In the following lemma, we present an upper bound for the Hausdorff distance between the attainability sets of conservative and non-conservative networks.

[5]Note that for linear systems the attainability sets for open and closed-loop control are the same.

Lemma 9. *The Hausdorff distance between the attainability sets of conservative and non-conservative networks, indicated by $\mathcal{S}_{\rm c}$ and $\mathcal{S}_{\rm nc}$ respectively, can be upper bounded as*

$$\begin{aligned} &h(\mathcal{S}_{\rm c}(t), \mathcal{S}_{\rm nc}(t)) \\ &\leq \sup_{m \in \mathcal{M}_0} \|m\| \|A - B\|_{\rm F} + \sup_{u \in \mathcal{U}} \|u\| \|C - D\|_{\rm F}\,, \end{aligned} \tag{53}$$

with $\|\cdot\|_{\rm F}$ the Frobenius norm, and where $A^{\rm T} = e^{tQ_{\rm c}}$, $B^{\rm T} = e^{tQ_{\rm nc}}$,

$$C^{\rm T} = \begin{cases} Q_{\rm c}^{-1}(e^{tQ_{\rm c}} - I_n) & \textit{for } Q_{\rm c} \textit{ nonsingular}\,, \\ t\sum_{k=0}^{\infty} \frac{1}{k+1} \frac{t^k Q_{\rm c}^k}{k!} & \textit{for } Q_{\rm c} \textit{ singular} \end{cases} \tag{54}$$

and

$$D^{\rm T} = \begin{cases} Q_{\rm nc}^{-1}(e^{tQ_{\rm nc}} - I_n) & \textit{for } Q_{\rm nc} \textit{ nonsingular}\,, \\ t\sum_{k=0}^{\infty} \frac{1}{k+1} \frac{t^k Q_{\rm nc}^k}{k!} & \textit{for } Q_{\rm nc} \textit{ singular}\,. \end{cases} \tag{55}$$

Proof: The support functions for conservative and non-conservative attainability sets are defined as

$$\begin{aligned} c(\mathcal{S}_{\rm c}(t), \psi) &= c\left(e^{(t-t_0)Q_{\rm c}} \mathcal{M}_0, \psi\right) + \int_{t_0}^{t} c\left(e^{(t-\tau)Q_{\rm c}} \mathcal{U}, \psi\right) {\rm d}\tau \\ c(\mathcal{S}_{\rm nc}(t), \psi) &= c\left(e^{(t-t_0)Q_{\rm nc}} \mathcal{M}_0, \psi\right) + \int_{t_0}^{t} c\left(e^{(t-\tau)Q_{\rm nc}} \mathcal{U}, \psi\right) {\rm d}\tau\,, \end{aligned} \tag{56}$$

where the property has been used that $c(\int_{t_0}^t e^{(t-\tau)Q} \mathcal{U} {\rm d}\tau, \psi) = \int_{t_0}^t c\left(e^{(t-\tau)Q} \mathcal{U}, \psi\right) {\rm d}\tau$. We bear on the following property of the Hausdorff metric to characterize the difference between the respective attainability sets

$$h(\mathcal{S}_{\rm c}(t), \mathcal{S}_{\rm nc}(t)) = \max_{\psi \in \mathcal{B}_n(0,1)} \left| c(\mathcal{S}_{\rm c}(t), \psi) - c(\mathcal{S}_{\rm nc}(t), \psi) \right|\,. \tag{57}$$

Assuming that $t_0 = 0$, we can write

$$\begin{aligned} c(\mathcal{S}_{\rm c}(t), \psi) - c(\mathcal{S}_{\rm nc}(t), \psi) &= c\left(e^{tQ_{\rm c}} \mathcal{M}_0, \psi\right) - c\left(e^{tQ_{\rm nc}} \mathcal{M}_0, \psi\right) \\ &+ \int_0^t \left[c\left(e^{(t-\tau)Q_{\rm c}} \mathcal{U}, \psi\right) - c\left(e^{(t-\tau)Q_{\rm nc}} \mathcal{U}, \psi\right)\right] {\rm d}\tau\,. \end{aligned} \tag{58}$$

For the integral term in (58) we find

$$\begin{aligned} &\int_0^t \left[c\left(\sum_{k=0}^{\infty} (t-\tau)^k \frac{Q_{\rm c}^k}{k!} \mathcal{U}, \psi \right) - c\left(\sum_{k-0}^{\infty} (t-\tau)^k \frac{Q_{\rm nc}^k}{k!} \mathcal{U}, \psi \right) \right] {\rm d}\tau \\ &= \sum_{k=0}^{\infty} \int_0^t (t-\tau)^k {\rm d}\tau \left[c\left(\frac{Q_{\rm c}^k}{k!} \mathcal{U}, \psi \right) - c\left(\frac{Q_{\rm nc}^k}{k!} \mathcal{U}, \psi \right) \right]\,, \end{aligned} \tag{59}$$

which can be solved as

$$c\left(Q_{\mathrm{c}}^{-1}\left(e^{tQ_{\mathrm{c}}}-I_n\right)\mathcal{U},\psi\right)-c\left(Q_{\mathrm{nc}}^{-1}\left(e^{tQ_{\mathrm{nc}}}-I_n\right)\mathcal{U},\psi\right) \tag{60}$$

when Q_{c} and Q_{nc} are non-singular, and

$$c\left(t\sum_{k=0}^{\infty}\frac{1}{k+1}\frac{t^kQ_{\mathrm{c}}^k}{k!}\mathcal{U},\psi\right)-c\left(t\sum_{k=0}^{\infty}\frac{1}{k+1}\frac{t^kQ_{\mathrm{nc}}^k}{k!}\mathcal{U},\psi\right) \tag{61}$$

when Q_{c} and Q_{nc} are singular. Defining A, B, C and D as in Lemma 9, (54), and (55), the Hausdorff metric can now be bounded as follows

$$\begin{aligned}
h(\mathcal{S}_{\mathrm{c}}(t),\mathcal{S}_{\mathrm{nc}}(t)) &= \max_{\psi\in\mathcal{B}_n(0,1)}|c(\mathcal{S}_{\mathrm{c}}(t),\psi)-c(\mathcal{S}_{\mathrm{nc}}(t),\psi)| \\
&= \max_{\psi\in\mathcal{B}_n(0,1)}\big|c(A^{\mathrm{T}}\mathcal{M}_0,\psi)-c(B^{\mathrm{T}}\mathcal{M}_0,\psi) \\
&\qquad\qquad + c(C^{\mathrm{T}}\mathcal{U},\psi)-c(D^{\mathrm{T}}\mathcal{U},\psi)\big| \\
&= \max_{\psi\in\mathcal{B}_n(0,1)}\big|c(\mathcal{M}_0,A\psi)-c(\mathcal{M}_0,B\psi) \\
&\qquad\qquad + c(\mathcal{U},C\psi)-c(\mathcal{U},D\psi)\big| \\
&\leq \max_{\psi\in\mathcal{B}_n(0,1)}|c(\mathcal{M}_0,A\psi)-c(\mathcal{M}_0,B\psi)| \\
&\qquad\qquad + |c(\mathcal{U},C\psi)-c(\mathcal{U},D\psi)| \\
&\overset{(a)}{\leq} \max_{\psi\in\mathcal{B}_n(0,1)}\sup_{m\in\mathcal{M}_0}\|m\|\|(A-B)\psi\|+\sup_{u\in\mathcal{U}}\|u\|\|(C-D)\psi\| \\
&\overset{(b)}{\leq} \max_{\psi\in\mathcal{B}_n(0,1)}\|\psi\|\Bigg(\sup_{m\in\mathcal{M}_0}\|m\|\sqrt{\sum_{i,j}(A-B)_{ij}^2} \\
&\qquad\qquad + \sup_{u\in\mathcal{U}}\|u\|\sqrt{\sum_{i,j}(C-D)_{ij}^2}\Bigg) \\
&= \sup_{m\in\mathcal{M}_0}\|m\|\sqrt{\sum(A-B)_{ij}^2}+\sup_{u\in\mathcal{U}}\|u\|\sqrt{\sum(C-D)_{ij}^2}\,,
\end{aligned} \tag{62}$$

where (a) follows from the property of support functions that $|c(\mathcal{F},\psi_1)-c(\mathcal{F},\psi_2)|\leq\sup_{f\in\mathcal{F}}\|f\|\|\psi_1-\psi_2\|$, and where (b) follows from $\langle x,\psi\rangle\leq\|x\|\|\psi\|$. This concludes the proof. $\square$

The presented upper bound for the Hausdorff distance between the attainability sets of conservative and non-conservative networks provides us with a metric to compare the variation of network dynamics following from different update rules. Some special cases are listed here

(i) In the case of symmetric networks, we have $Q_{\mathrm{c}}=Q_{\mathrm{nc}}$. We find that $h(\mathcal{S}_{\mathrm{c}}(t),\mathcal{S}_{\mathrm{nc}}(t))=0$, such that $\mathcal{S}_{\mathrm{c}}(t)=\mathcal{S}_{\mathrm{nc}}(t)$, or the attainability set is the same for conservative and non-conservative network dynamics when the system matrix is symmetric.

(ii) In the case of networks with link directions inversed, we have $Q_{\mathrm{c}} = Q_{\mathrm{nc}}^{\mathrm{T}}$. In this case, it can be demonstrated easily that $B = A^{\mathrm{T}}$ and $D = C^{\mathrm{T}}$. The Hausdorff distance can in this case be upper bounded as

$$\begin{aligned} h(\mathcal{S}_{\mathrm{c}}(t), \mathcal{S}_{\mathrm{nc}}(t)) \leq \sup_{m \in \mathcal{M}_0} \|m\| \sqrt{\sum (A - A^{\mathrm{T}})_{ij}^2} \\ + \sup_{u \in \mathcal{U}} \|u\| \sqrt{\sum (C - C^{\mathrm{T}})_{ij}^2} \,. \end{aligned} \tag{63}$$

This formula reveals how the Hausdorff distance increases with the asymmetry of the network.

Apart from characterizing the Hausdorff distance between attainability sets, the support function is also very powerful for other purposes. We note here that the support function allows us to verify if sets intersect by applying

$$\mathcal{S}_{\mathrm{c}}(t) \cap \mathcal{S}_{\mathrm{nc}}(t) \neq \emptyset \Leftrightarrow c(\mathcal{S}_{\mathrm{c}}(t), \psi) + c(\mathcal{S}_{\mathrm{nc}}(t), -\psi) \geq 0, \, \forall \psi \in \mathbb{R}^n \,. \tag{64}$$

Furthermore, we can verify if $\mathcal{S}_{\mathrm{c}}(t) \subset \mathcal{S}_{\mathrm{nc}}(t)$, by applying

$$\mathcal{S}_{\mathrm{c}}(t) \subset \mathcal{S}_{\mathrm{nc}}(t) \Leftrightarrow c(\mathcal{S}_{\mathrm{c}}(t), \psi) \leq c(\mathcal{S}_{\mathrm{nc}}(t), \psi), \, \forall \psi \in \mathbb{R}^n \,. \tag{65}$$

Note that the verification of intersection and inclusion usually requires numerical analysis.

V. Network control by structure modification

Instead of controlling the network dynamics through exogenous excitation, which may not always be feasible, we can also steer the dynamics by modifying the network structure.

A. *Network structure modification through design*

Instead of controlling the system with an exogenous input term, we can also modify the network structure directly to achieve control. Modifying the network structure may be preferable to introducing external excitations in systems where it is more convenient to modify the interactions between agents than to introduce or remove property from agents. Through this modification, we can shift both the eigenvalues and the eigenvector components, thereby changing the system dynamics, characteristic timescales, as well as the stationary behavior. By modifying the links carefully, we can achieve modification of the characteristic timescales without reshaping the basis of system modes, which is composed by the eigenvectors. This is formulated in the following Lemma.

Lemma 10. *If the diagonal elements of* Λ *in the decomposition of a diagonalizable matrix* $Q = A\Lambda A^{-1}$ *are altered, then the resulting matrix* $\tilde{Q} = A\tilde{\Lambda}A^{-1}$ *has the same system modes and represents a CTMC, given that the eigenvalue* $q_{\mathrm{s}} = 0$ *is preserved and* $q_i < 0, \ \forall \ i \neq 1$.

Proof: Apart from decomposing Q into the matrices A, Λ and A^{-1}, we can also reconstruct Q by multiplying A, Λ and A^{-1} together in the appropriate order. By holding A constant and modifying the diagonal elements of Λ, we can achieve a modification in Q, represented by $\tilde{Q}$, without affecting the composition of the system modes. The stability of the new eigenvalues of the modified Q determines if $\tilde{Q}$ still represents a CTMC described by (A). With $q_{\mathrm{s}} = 0$ and $q_{\mathrm{s}} \in \sigma(\tilde{Q})$ where $\sigma(.)$ represents the spectrum of a matrix, the columns and rows of $\tilde{Q}$ will still sum to zero for conservative and non-conservative networks, respectively. Hence, $\tilde{Q}$ represents the transition rate matrix of a CTMC. □

To illustrate how we can modify the eigenvalues of a network to achieve a shift in the system response, we consider a symmetric star network depicted in Fig. 5. The transition rate matrix Q corresponding to this network is

$$Q = \begin{bmatrix} -4 & 1 & 1 & 1 & 1 \\ 1 & -1 & 0 & 0 & 0 \\ 1 & 0 & -1 & 0 & 0 \\ 1 & 0 & 0 & -1 & 0 \\ 1 & 0 & 0 & 0 & -1 \end{bmatrix}.$$

The eigenvalues of this matrix are 0 with multiplicity 1, -5 with multiplicity 1 and -1 with multiplicity 3. The corresponding eigenvectors are the steady-state eigenvector describing equilibration between all the nodes ($\begin{bmatrix} 1 & 1 & 1 & 1 & 1 \end{bmatrix}$), an eigenvector describing diffusion between the peripheral nodes and the central node ($\begin{bmatrix} -4 & 1 & 1 & 1 & 1 \end{bmatrix}$), and eigenvectors describing diffusion among the peripheral nodes ($\begin{bmatrix} 0 & 1 & 1 & 1 & -3 \end{bmatrix}$, $\begin{bmatrix} 0 & 0.36 & 1 & -1.36 & 0 \end{bmatrix}$ and $\begin{bmatrix} 0 & -1.36 & 1 & 0.36 & 0 \end{bmatrix}$). Suppose we want to slow down diffusion between the peripheral nodes and the central node. We can do so by decreasing the effective update rate of this mode, which causes the relative importance of diffusion among

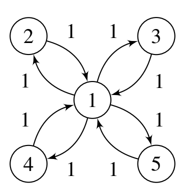

Fig. 5: Star graph S_5 with symmetric links of unit weights.

the peripheral nodes to increase and results in extra links facilitating this diffusion. For instance, by changing the effective update rate of the peripheral-central mode from 5 to 4.5, we obtain the following transition rate matrix

$$Q = \begin{bmatrix} -3.6 & 0.9 & 0.9 & 0.9 & 0.9 \\ 0.9 & -0.975 & 0.025 & 0.025 & 0.025 \\ 0.9 & 0.025 & -0.975 & 0.025 & 0.025 \\ 0.9 & 0.025 & 0.025 & -0.975 & 0.025 \\ 0.9 & 0.025 & 0.025 & 0.025 & -0.975 \end{bmatrix}.$$

In the resultant architecture, the links between the central node and the peripheral nodes have weights of 0.9 instead of 1, and the links between the peripheral nodes have weights of 0.025 instead of 0. The corresponding network is a superposition of the two graphs depicted in Fig. 6.

B. Network structure modification through adaptive control

In sufficiently large systems, it can be computationally intensive to perform the eigendecomposition of various Q matrices in order to determine the network structure that gives the most desirable system response. Moreover, it is often not straightforward to translate network objectives, both dynamic and in steady-state, into an appropriate eigendecomposition. There are two possible approaches to handle this issue. Firstly, we can choose from a set of matrices that deviate from the original Q by small perturbations δQ. The eigenvalue and eigenvector perturbations can be derived as a function of δQ for sufficiently small δQ. However, this limits us to small modifications in the network structure that do not span the feasible action space, and potentially more desirable network structures may not be explored by this approach. Nevertheless, it is possible to examine larger modifications without going through the computational complexity by performing adaptive control driven by reinforcement learning.

In the approach based on adaptive control, we formulate the problem as an MDP. The state space of the MDP is equivalent to the node space $\mathcal{V}$ of the network, while the action space $\mathcal{W}$

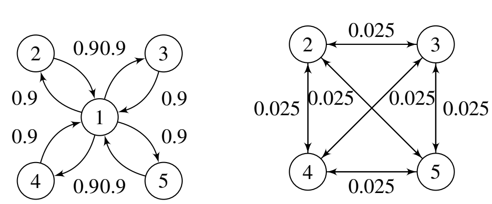

Fig. 6: The superposition of these two graphs yields the network structure corresponding to the modified transition rate matrix given in (66).

of the MDP is equivalent to the set of possible Q matrices that the network can adopt. More formally, $\mathcal{W} = \{Q_1, \ldots, Q_w\}$ for w different actions. In essence, the MDP is a direct extension of the CTMC upon which the governing equation of the network dynamics is based. By selecting a reward function $R(X, Q)$ that describes the desirability of action Q given that the system is in state X, and by scheduling decisions to be made immediately after a change of the network state[6], the MDP is completely defined. The solution to the MDP gives us the most desirable network structure, which is obtained by picking the most highly rewarded incoming or outgoing link weights for each node. The conditions for optimality in the MDP can be determined by searching the policy that yields the maximum expected reward integrated over time

$$\mathbb{E}_{X_0,Q(0),\text{ sample paths}}\left[\int_0^\infty \gamma^t R(X(t), Q(t))\mathrm{d}t\right], \tag{66}$$

where $\gamma \in (0, 1)$ denotes a discount rate. By considering (A) and (66) simultaneously, we obtain the Hamilton-Jacobi-Bellman equation for the system. In optimal control theory, this equation is solved to obtain the optimal policy for the system. For large state and/or action spaces, the solution to this problem is difficult to obtain. For a more computationally manageable approach, we turn to reinforcement learning to determine a suboptimal solution with sufficiently fast convergence. For each state-action pair (X, Q), we store a quality value $V^{(\mathrm{q})}(X, Q)$, and update $V^{(\mathrm{q})}(X, Q)$ based on the Q-learning method [23]

$$\begin{aligned} V^{(\mathrm{q})}_{k+1}(X_k, Q_k) &= (1-\mu)V^{(\mathrm{q})}_k(X_k, Q_k) \\ &\quad + \mu\left[\max_{Q\in\mathcal{W}} R(X_{k+1}, Q) + \gamma \max_{Q\in\mathcal{W}} V^{(\mathrm{q})}_k(X_{k+1}, Q)\right], \end{aligned} \tag{67}$$

where k is the index indicating the k-th change of the system state, $\mu \in (0, 1]$ is the learning rate of the algorithm, and X_k is state vector after k changes of the system. Whenever the system transitions to a new state, a new action has to be selected. We set up the system such that with probability ϵ, the system selects the action with the highest quality given its current state, while with probability $1-\epsilon$ the system selects a random action. This is known as the ϵ-greedy policy where ϵ is the exploitation probability of the system. By selecting appropriate values of μ, γ and ϵ, as well as an appropriate reward function $R(X, Q)$, we can design the learning process to achieve predefined network objectives at a suitable convergence rate. In other words, the reinforcement learning algorithm can offer us a well-performing network structure within a reasonable amount of time by searching a reasonable portion of the total space of

[6]This means that the variation of the active action $Q(t)$ with time is a piecewise constant function.

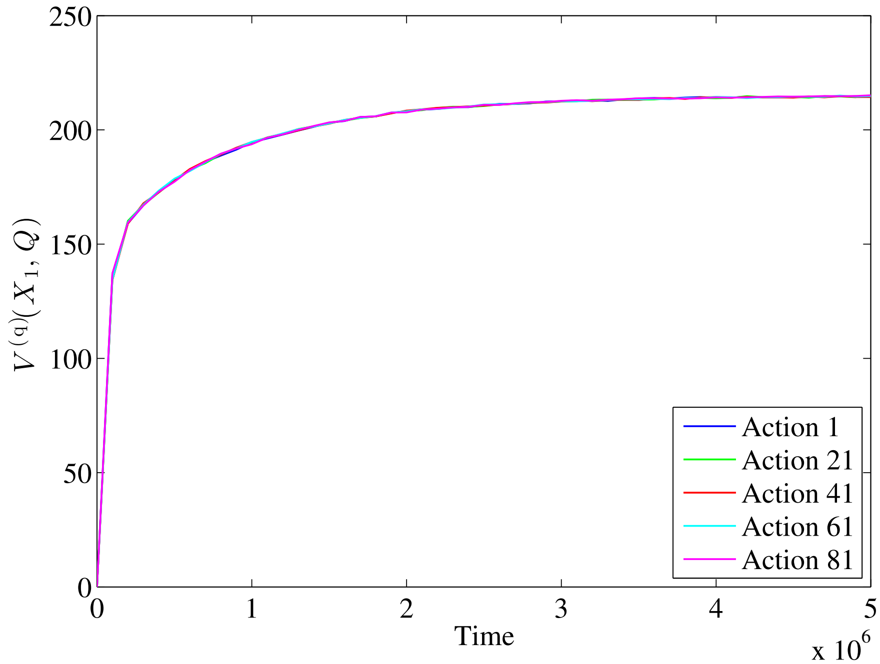

Fig. 7: Time evolution of quality $V^{(\mathrm{q})}(X_1, Q)$ for 5 different actions Q for a single trial.

available actions. The performance of a similar learning algorithm was recently examined in a CTMC-based duty cycling framework [35].

To illustrate the use of an MDP to select a desirable Q in a large network, we set up a network and corresponding state space containing 20 agents. We also set up the action space $\mathcal{W}$ by generating 400 Q matrices corresponding to 400 complete graphs whose links each have weights sampled from a uniform distribution on $[0, 1]$, to simulate 400 different random network configurations. These matrices obey the conservative relation (12) according to (P1). In addition, we select 2 arbitrary nodes (12 and 14) out of the 20 to serve as target nodes for our system. We let the state transitions of the MDP be governed by a grand system transition matrix Q_{g}. Whenever a state transition occurs, we assign a reward of 5 whenever the state coincides with 1 of these 2 target nodes, and a reward of 0 otherwise, in order to encourage the system to visit these states more often. The MDP then selects an action, following which Q_{g} is updated based on this selected action. For example, if the updated state of the system is node 5 and action 20 is selected, then the 5th column of Q_{g} is replaced by the 5th column of Q_{20} corresponding to the 20th action. This means that the incoming link weights of node 5 are updated to those corresponding to the 20th Q matrix. For this work, we ran 100 independent numerical simulations describing the time evolution of 100 MDPs with the same state and action spaces, but with different initial

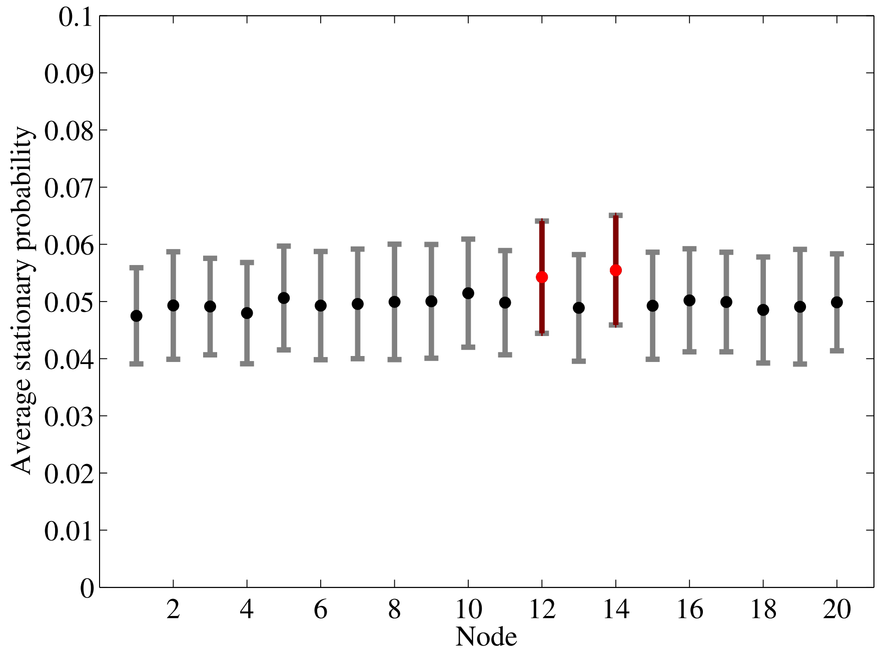

Fig. 8: Stationary probability distribution of the simulated network averaged over 100 trials. The nodes marked red are the two randomly selected nodes (12 and 14) that were assigned a reward on every visit by each MDP.

states S_0 and actions $Q_{\rm g}(0)$. Using the reinforcement learning parameters $\mu = 0.2$, $\epsilon = 0.4$ and $\gamma = 0.995$, we run each simulation for 5E6 time-steps, following which we find the steady-state eigenvector (normalized to sum to 1), or stationary distribution, $v_{\rm R,s}$ for each last known $Q_{\rm g}$ such that $Q_{\rm g} v_{\rm R,s} = 0$ and $\sum_i v_{\rm R,s}(i) = 1$. In Fig. 7, we demonstrate using the time evolution of $V^{(\rm q)}(X_1, Q)$ for 5 different actions Q that the learning curve has reached convergence. In Fig. 8, we plot the last known stationary distribution $v_{\rm R,s}(i)$ over all the states i averaged over the 100 trials, and demonstrate that the MDP is, on average, able to modify the stationary distribution of the system after sufficient time has elapsed by careful design of the reward function. In this case, we guided the system to favor nodes 12 and 14 by modifying the network structure. This MDP methodology can either be used online to allow the network to respond to time-varying objectives, or offline to cycle through various network possibilities with reduced computational complexity.

VI. Conclusion

In this work, we proposed a probabilistic framework that represents the dynamics in multi-agent networks subject to two protocols with constant and variable total network quantity. By including the possibility of asymmetric updates, weighted links and switching topologies, we examined the general stability and temporal dynamics in conservative and non-conservative networks. Furthermore, we demonstrated the ability to achieve network control using either external excitation or modification of the network structure. Our framework allows to study individual trajectories in terms of the dynamical and stationary properties. In particular, we stated the exact role of the network structure, the update rule, and the external excitation in the characteristics of the controlled output. In addition, we presented a method to analyze the set of trajectories under control constraints by examining the set of attainability. We presented a method based on the support function to measure the difference between attainability sets of networks that operate under different protocols. As to the modification of the network structure, we presented an algorithm involving reinforcement learning to obtain networks with a desired behavior. Through these techniques, we enabled the micromanagement of the dynamics that take place over multi-agent networks. Our future work will include applications to large-scale random networks, and cover time-inhomogeneous and stochastic governing equations. Another important extension is to develop more insight in the higher order moments of the property.

References

[1] W. H. R. Chan, M. Wildemeersch, and T. Q. S. Quek, "Diffusion control in multi-agent networks," in *IEEE Conference on Decision and Control (CDC)*, 2015, pp. 4190–4195.

[2] A. Jadbabaie, J. Lin, and A. S. Morse, "Coordination of groups of mobile autonomous agents using nearest neighbor rules," *IEEE Trans. Automat. Contr.*, vol. 48, no. 6, pp. 988–1001, 2003.

[3] A. G. Dimakis, S. Kar, J. M. Moura, M. G. Rabbat, and A. Scaglione, "Gossip algorithms for distributed signal processing," *Proc. of the IEEE*, vol. 98, no. 11, pp. 1847–1864, 2010.

[4] K. Kandhway and J. Kuri, "Campaigning in heterogeneous social networks: Optimal control of SI information epidemics," *IEEE/ACM Trans. Netw.*, 2014, early access.

[5] F. Pasqualetti, S. Zampieri, and F. Bullo, "Controllability metrics, limitations and algorithms for complex networks," *IEEE Trans. Control Netw. Syst.*, vol. 1, no. 1, pp. 40–52, Mar. 2014.

[6] J. Chen and A. H. Sayed, "Distributed pareto optimization via diffusion strategies," *IEEE J. Sel. Topics Signal Process.*, vol. 7, no. 2, pp. 205–220, 2013.

[7] D. Acemoglu and A. Ozdaglar, "Opinion dynamics and learning in social networks," *Dynamic Games and Applications*, vol. 1, no. 1, pp. 3–49, 2011.

[8] E. Mallada, R. Freeman, *et al.*, "Distributed synchronization of heterogeneous oscillators on networks with arbitrary topology," *IEEE Trans. Control Netw. Syst.*, 2015, early access.

[9] V. Blondel, J. M. Hendrickx, A. Olshevsky, and J. Tsitsiklis, "Convergence in multiagent coordination, consensus, and flocking," in *IEEE Conference on Decision and Control, and the European Control Conference*, Seville, Spain, Dec. 2005, p. 2996.

[10] Q. Ren and H. Kobayashi, "Diffusion approximation modeling for Markov modulated bursty traffic and its applications to bandwidth allocation in ATM networks," *IEEE J. Sel. Areas Commun.*, vol. 16, no. 5, pp. 679–691, 1998.

[11] M. E. Yildiz, A. Scaglione, and A. Ozdaglar, "Asymmetric information diffusion via gossiping on static and dynamic networks," in *Proc. of the IEEE Conference on Decision and Control*, Atlanta, GA, USA, Dec. 2010, pp. 7467–7472.

[12] G. Como, K. Savla, D. Acemoglu, M. A. Dahleh, and E. Frazzoli, "Robust distributed routing in dynamical flow networks," in *IEEE Conf. on Decision and Control and European Control Conference (CDC-ECC)*, Orlando, FL, USA, Dec. 2011, pp. 6290–6295.

[13] J. Kiessling and R. Tempone, "Diffusion approximation of Lévy processes with a view towards finance," *Monte Carlo Methods and Applications*, vol. 17, no. 1, pp. 11–45, 2011.

[14] D. Acemoglu, G. Como, F. Fagnani, and A. Ozdaglar, "Opinion fluctuations and disagreement in social networks," *Mathematics of Operations Research*, vol. 38, no. 1, pp. 1–27, 2013.

[15] D.-W. Tcha and S. R. Pliska, "Optimal control of single-server queuing networks and multi-class M/G/1 queues with feedback," *Operations Research*, vol. 25, no. 2, pp. 248–258, 1977.

[16] R. Olfati-Saber and R. M. Murray, "Consensus problems in networks of agents with switching topology and time-delays," *IEEE Trans. Automat. Contr.*, vol. 49, no. 9, pp. 1520–1533, 2004.

[17] R. Olfati-Saber, J. A. Fax, and R. M. Murray, "Consensus and cooperation in networked multi-agent systems," *Proc. of the IEEE*, vol. 95, no. 1, pp. 215–233, 2007.

[18] D. Acemoglu, A. Nedic, and A. Ozdaglar, "Convergence of rule-of-thumb learning rules in social networks," in *IEEE Conference on Decision and Control*, Cancun, Mexico, Dec. 2008, pp. 1714–1720.

[19] A. Banerjee and J. Jost, "On the spectrum of the normalized graph laplacian," *Linear algebra and its applications*, vol. 428, no. 11, pp. 3015–3022, 2008.

[20] Y. Hong, J. Hu, and L. Gao, "Tracking control for multi-agent consensus with an active leader and variable topology," *Automatica*, vol. 42, no. 7, pp. 1177–1182, 2006.

[21] M. Ji, G. Ferrari-Trecate, M. Egerstedt, and A. Buffa, "Containment control in mobile networks," *IEEE Trans. Automat. Contr.*, vol. 53, no. 8, pp. 1972–1975, 2008.

[22] S. Brin and L. Page, "The anatomy of a large-scale hypertextual web search engine," *Computer networks and ISDN systems*, vol. 30, no. 1-7, pp. 107–117, 1998.

[23] A. G. Barto and R. S. Sutton, *Reinforcement learning: An introduction*. MIT Press, 1998.

[24] R. Olfati-Saber and R. M. Murray, "Consensus protocols for networks of dynamic agents," in *Proc. Amer. Control Conf.*, Denver (CO), USA, Jun. 2003, pp. 951–956.

[25] P. Van Mieghem, *Performance analysis of communications networks and systems*. Cambridge University Press, 2006.

[26] M. Thompson, R. Ellis, and A. Wildavsky, *Cultural theory.* Westview Press, 1990.

[27] A. Tversky and D. Kahneman, "Availability: A heuristic for judging frequency and probability," *Cognitive psychology*, vol. 5, no. 2, pp. 207–232, 1973.

[28] D. Shemesh, "Common eigenvectors of two matrices," *Linear algebra and its applications*, vol. 62, pp. 11–18, 1984.

[29] L. Farina and S. Rinaldi, *Positive linear systems: theory and applications*. John Wiley & Sons, 2011, vol. 50.

[30] K. Lerman and R. Ghosh, "Information contagion: An empirical study of the spread of news on digg and twitter social networks." 2010.

[31] J. C. Willems, "Lyapunov functions for diagonally dominant systems," *Automatica*, vol. 12, no. 5, pp. 519–523, 1976.

[32] E. B. Lee and L. Markus, *Foundations of Optimal Control Theory*. Krieger, 1967.

[33] A. B. Kurzhanskiĭ and I. Vályi, *Ellipsoidal calculus for estimation and control*. Birkhäuser, 1997.

[34] R. T. Rockafellar, *Convex Analysis*. Princeton University Press, 1970.

[35] W. H. R. Chan, P. Zhang, I. Nevat, S. G. Nagarajan, A. C. Valera, H.-X. Tan, and N. Gautam, “Adaptive duty cycling in sensor networks with energy harvesting using continuous-time markov chain and fluid models,” *IEEE Journal on Selected Areas in Communications*, vol. 33, no. 12, pp. 2687–2700, 2015.